



# Low energy collisions between ground-state oxygen atoms

C. Tully\*, R.E. Johnson

*Department of Engineering Physics and Astronomy, Thornton Hall, University of Virginia, Charlottesville, VA 22903, USA*

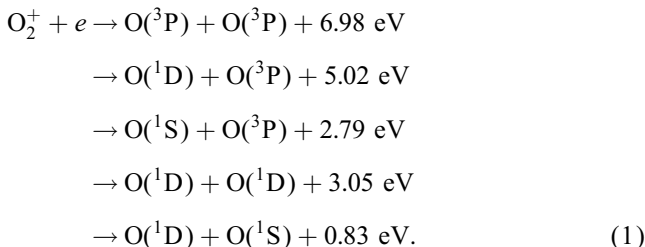
Received 11 September 2000; accepted 15 November 2000

## Abstract

Elastic scattering cross sections have been calculated for the  $O(^3P) + O(^3P)$  collision at energies  $E = 1\text{--}10$  eV using exact quantum calculations and the semiclassical Jeffries–Wentzel–Kramers–Brillouin approximation with the full set of 18 states of  $O_2$  which separate to this system. These cross sections are required for calculating escape probability from planetary atmospheres. In addition, an average potential has been calculated and compared to popularly used potential energy forms. The average potential has also been used to generate the cross sections in this energy range. Escape depths for  $E = 1$  and 10 eV have been calculated to be  $1.0 \times 10^{15}$  and  $2.5 \times 10^{14}/\text{cm}^2$ , respectively. © 2001 Elsevier Science Ltd. All rights reserved.

## 1. Introduction

Bombardment of an atmosphere by energetic ions and dissociative recombination of atmospheric molecular ions produce energetic recoil atoms. These can heat the thermosphere and can lead to escape from the planet affecting the evolution of the atmosphere (Hunten et al., 1989). For instance, dissociative recombination of  $O_2^+$  produces two energetic O atoms, each of which leads to a cascade of collisions, an important heating process in the thermospheres of Venus, Earth and Mars. It can occur through the following channels (Fox and Bougher, 1991):



If the kinetic energy on the right is twice the escape energy and the recombination process occurs near the exobase one of the O atoms can escape, a process important at Mars and Europa (Johnson et al., 1998). Similarly an incident energetic ion produces recoil atoms which initiate collision cascades. These also heat the thermosphere and

set some O atoms on escape trajectories (e.g. Johnson, 1990, 1994).

Determining the escape probability requires accurate cross sections for the collision of the energized O atom with the ambient atoms and molecules. Since the thermospheres of Venus and Earth near the exobase are dominated by O, as is the thermosphere of Mars in earlier epochs (Zhang et al., 1993), accurate cross sections are needed for O atoms colliding with ground-state O. Yee and Dalgarno (1985) and Yee et al. (1990) have calculated the elastic and quenching cross sections for  $O(^1D)$  colliding with  $O(^3P)$ . However, accurate cross sections for collisions between ground-state atoms,  $O(^3P) + O(^3P)$ , have not been calculated. When such values are required, a hard sphere cross section of about  $2 \times 10^{-15}/\text{cm}^2$  was assumed (Paxton, 1985; Nagy et al., 1981).

In this paper we calculate the angular differential cross sections, the total elastic cross sections and the diffusion cross sections of a ground-state  $O(^3P)$  atom in collision with another  $O(^3P)$  atom in the energy range from 1 to 10 eV, which is the region of interest for determining the escape probability from a number of planetary atmospheres. These results are then compared to popularly used approximate models.

## 2. Calculations

To escape from a planetary atmosphere a particle moving upward from the exobase with a velocity greater than the escape velocity must have a probability significantly

\* Corresponding author. Tel.: +1-804-243-8943; fax: +1-804-924-1353.

E-mail address: ct5q@virginia.edu (C. Tully).

less than 1 of being deflected during a collision with another atom. The probability of such a collision is determined from a cross section,  $\sigma$ , and the total number density,  $n$ . The exobase is typically defined as the planetary altitude at which the mean free path  $\lambda_c [= (n\sigma)^{-1}]$  is equal to the atmospheric scale height  $H [= kT/mg]$ . This criterion,  $H = \lambda_c$ , implies that the escape probability is  $e^{-1}$ . This also means that the line-of sight column density above the exobase ( $nH$ ) is equal to  $\sigma^{-1}$ . For Jeans escape the total elastic cross section, which we write as  $\sigma$ , is often used to define the exobase (Chamberlain and Hunten, 1987). However, the diffusion (momentum transfer) cross section,  $\sigma_d$ , is probably more appropriate. For a flat atmosphere, the exobase column density has been estimated to be  $c/\sigma_d$ , with  $c \approx 1.3$  for 1 eV atoms using a steep repulsive potential (Johnson, 1994). Therefore, we calculate here the cross sections for deflection of an O atom as well as the total elastic and the diffusion cross sections.

In calculating the cross sections for  $O(^3P) + O(^3P)$  all 18 molecular symmetry states of  $O_2$  which separate to this collision pair must be taken into account. The average differential scattering cross section,  $\sigma(\chi)$ , at each center of mass energy  $E$ , for the system is calculated as the weighted sum of the individual differential cross sections  $\sigma_j(\chi)$  for each state  $j$ ,

$$\sigma(\chi) = \sum_j g_j \sigma_j(\chi) = \sum_j g_j |f_j(\chi)|^2, \quad (2)$$

where  $j$  is a label indicating the molecular state,  $\chi$  is the center of mass scattering angle and  $g_j$  is the statistical weight. The quantity  $f_j(\chi)$  is the scattering amplitude and is determined by (Bransden and Joachain, 1983)

$$f_j(\chi) = \frac{1}{2ik} \sum_{l=0}^{\infty} (2l+1) \{ \exp(2i\eta_l^j) - 1 \} P_l(\cos \chi), \quad (3)$$

where  $\eta_l^j$  are the phase shifts,  $k [= \sqrt{2mE/\hbar}]$  is the wave number, the  $P_l(\cos \chi)$  are the Legendre polynomials,  $l$  is an index related to the angular momentum and  $i = \sqrt{-1}$ .

Using the average differential cross section, the momentum transfer or diffusion cross section for each state can be determined by

$$(\sigma_d)_j = 2\pi \int_{-\pi}^{\pi} \sigma_j(\chi) (1 - \cos \chi) \sin \chi d\chi. \quad (4)$$

By substituting Eqs. (3) and (4) into the above expression, the diffusion cross section can be calculated from the phase shifts as a sum over angular momentum index  $l$ ,

$$(\sigma_d)_j = \frac{4\pi}{k^2} \sum_{l=0}^{\infty} (l+1) \sin^2(\eta_{l+1}^j - \eta_l^j) \quad (5)$$

and the average diffusion cross section will be given by

$$\sigma_d = \sum_j g_j (\sigma_d)_j. \quad (6)$$

Similarly, the average total elastic cross section can be determined from

$$\sigma = \sum_j \sigma_j = \frac{2\pi}{k^2} \sum_{l=0}^{\infty} (2l+1) \sin^2(\eta_l^j), \quad (7)$$

where  $\sigma_j$  is the total elastic cross section for each state.

The integrated cross sections above can be related to classical cross sections by assuming the classical impact parameter,  $b$ , is  $(l + \frac{1}{2})/k$ . Further, when describing the cascade of collisions initiated by an energetic recoil atom, the cross section for energy transfer,  $[d\sigma/dT]$ , is often used instead of the angular differential cross section. Here  $T$  is the energy transferred from an atom of energy  $E_O$  to a stationary atom. These two cross sections are simply related (Johnson, 1982, 1990) [i.e., for collisions between atoms,  $d\sigma/dT = 4\pi\sigma(\chi)/\gamma E_O$ , with  $T = \gamma E_O/2(1 - \cos \chi)$  and the mass factor,  $\gamma = 1$ , for O on O]. In addition, the diffusion cross section is simply related to the elastic (nuclear) stopping cross section,  $S_n$ , often used in particle penetration studies [i.e.,  $S_n = (\gamma E_O/2)\sigma_d$ ].

The phase shifts are obtained by numerically solving the radial Schrödinger equation

$$\frac{d^2 F_l^j(r)}{dr^2} + \left( k^2 - 2\mu V_j(r) - \frac{l(l+1)}{r^2} \right) F_l^j(r) = 0, \quad (8)$$

where  $\mu$  is the reduced mass, subject to the boundary conditions

$$F_l^j(r \rightarrow 0) = \sum_{i=0}^{\infty} a_i^j r^{l+i+1}, \quad (9)$$

where  $a_i^j$  are constants, and

$$F_l^j(r \rightarrow \infty) \approx \sin(kr - l\pi/2 + \eta_l^j). \quad (10)$$

Here  $V_j(r)$  is the interaction potential corresponding to a particular molecular state.

The interaction potentials for the molecular states of  $O_2$  which separate to give  $O(^3P) + O(^3P)$  used are the calculated results of Saxon and Lui (1977) for the range  $r = 1.8a_0 - 20a_0$ . Since the repulsive part of the potential needs to be defined everywhere in order to solve Eq. (8), for  $r < 1.8a_0$  it is obtained by fitting the data to a potential of the form

$$V_j(r) = \frac{A_j e^{-\alpha_j r}}{r} \quad \text{for } r < 1.8a_0, \quad (11)$$

where  $A_j$  and  $\alpha_j$  are constant values calculated for each potential curve. For three of the lowest states,  $b^1\Sigma_g^+$ ,  $a^1\Delta_g$  and  $X^3\Sigma_g^-$ , this potential energy form forces the potential to rise towards infinity much too quickly. To avoid this steep ascent to infinity and any potential curve crossing with states of the same symmetry, the repulsive interaction potential of these three states was fitted to the form

$$V_j(r) = \frac{A_j e^{-\alpha_j r}}{r} + \frac{B_j}{r} \quad \text{for } r < 1.8a_0, \quad (12)$$

where  $A_j$ ,  $B_j$  and  $\alpha_j$  are constants associated with each state. Varying these forms does not change the cross sections significantly in the energy region of interest. At large

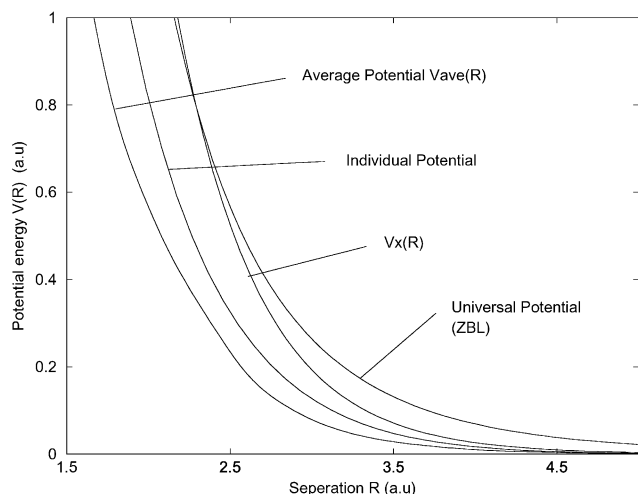


Fig. 1. Potential energy curves of O + O calculated using the average potential, the universal potential (ZBL), the ‘individual’ potential and a Born–Mayer form,  $V_x(R)$ .

separations, the potential is fitted to the long-range van der Waals form (Konowalow et al., 1959)

$$V_j(r) = \frac{-11.7}{r^6} \quad \text{for } r > 20a_0, \quad (13)$$

where  $V_j(r)$  is in atomic units (27.2116 eV) and  $r$  is in  $a_0$ . Having extrapolated the potentials we solved Eq. (8) using a Runge–Kutta integration and extracted the phase shift by fitting the result at large  $r$  to the form in Eq. (10).

Due to the effort involved in calculating potentials and cross sections for all 18 states and then finding an average cross section, an average effective potential is often used in describing low-energy collision cascades. These are typically semi-empirical potentials. Using the 18 Saxon and Lui potentials for ground-state O + O, an ‘average’ potential,  $V_{ave}(r)$ , can be constructed by summing the weighted interaction potentials for each state,

$$V_{ave}(r) = \sum_j g_j V_j(r). \quad (14)$$

This process has been shown to lead to incorrect differential cross sections at low energies if the potentials differ significantly (Johnson et al., 1972), but is acceptable in the repulsive regime at small  $r$ . A better procedure is to extract an effective potential from the measured differential cross section. The average potential in Eq. (14) is illustrated in Fig. 1 along with a ‘universal’ potential (ZBL potential), which was calculated by Zeigler et al. (1985) from a fit to a large amount of atomic cross section data for a variety of collision pairs. This scaled potential is often used to estimate atomic interaction potentials. Another potential form known as the ‘individual’ potential, shown to be in better agreement with the calculated average potential as illustrated in Fig. 1, is given by Gärtner and Hehl (1979) using a theoretical screening function. Finally, we also show a simple exponential potential, often called a Born–Mayer potential, given by  $V_x(r) = A_x \exp(-r/a_x)$ . The parameters

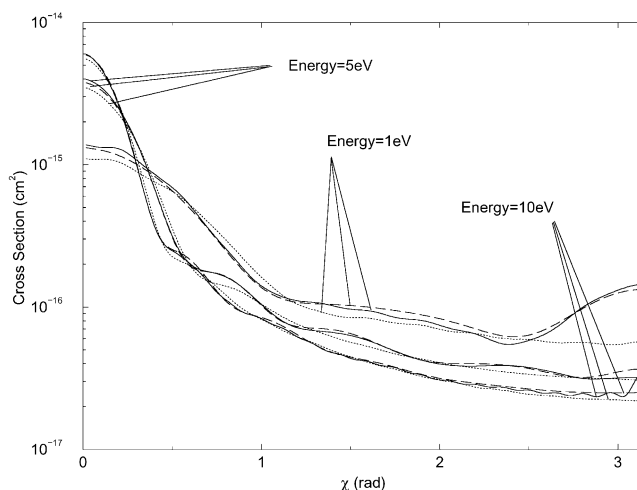


Fig. 2. Differential cross section at relative energies  $E = 1, 5$  and  $10$  eV calculated using the exact quantum phase shifts (solid lines), the semi-classical phase shifts (dashed lines) and the exact phase shifts for the average potential (dotted lines).

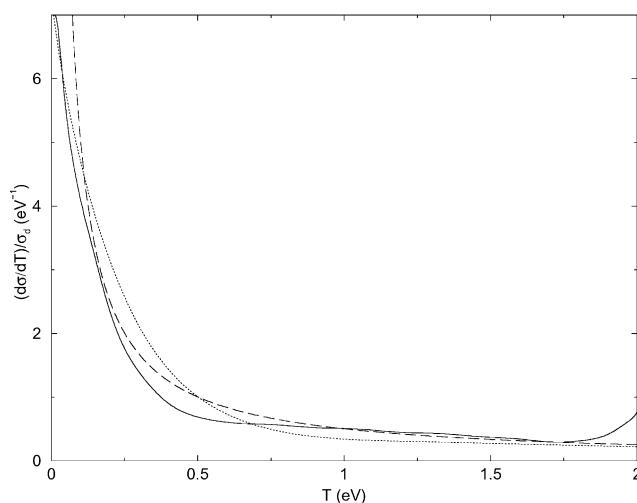


Fig. 3. Average differential cross sections given in the form  $(d\sigma/dT)/\sigma_d$  vs.  $T$  for relative energy  $E = 1$  eV (solid line) and  $E = 10$  eV (dotted line). Also shown by the dashed line is the steeply repulsive form  $d\sigma/dT = C/T$  often used in sputtering divided by  $\sigma_d$  with  $C = \sigma_d/2$ .

have been extracted from low-energy data (Foreman et al., 1976),  $A_x = 2143$  eV and  $a_x = 0.2604$  Å for O atoms in collision with O.

$V_{ave}(r)$  has also been used to calculate the phase shifts and determine the total elastic cross section, the diffusion cross section and the average differential cross section. In Figs. 2–4 these results are compared to those obtained using the exact phase shifts in Eqs. (2), (6) and (7).

### 3. Results

The differential cross sections for each state can exhibit considerable structure and even rainbows for low-energy collisions in the lowest molecular state. However, the

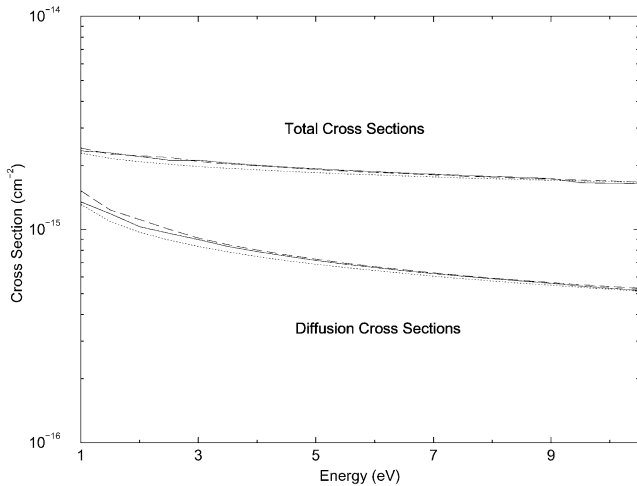


Fig. 4. Total integrated cross sections and diffusion cross sections for collisions of  $O(^3P)$  on  $O(^3P)$  calculated using the exact quantum phase shifts (solid lines), the semi-classical phase shifts (dashed lines) and the exact phase shifts for the average potential (dotted lines).

average differential cross section from Eq. (2) has little structure. Fig. 2 shows the average differential cross sections for relative energies  $E=1, 5$  and  $10$  eV, respectively, determined using the exact phase shifts (solid lines) and the weights for each state, calculated as described above. For comparison the semiclassical Jeffries–Wentzel–Kramers–Brillouin (JWKB) phase shifts  $\delta_l^j$ , given by (Joachain, 1975)

$$\delta_l^j = (l + 1/2)\pi/2 - kr_0 + \int_{r_0}^{\infty} [(U_l^j(r))^{1/2} - k] dr, \quad (15)$$

where  $U_l^j(r) = k^2 - 2\mu V_j(r) - (l(l+1))/r^2$  and  $r_0$ , the distance of closest approach, occurs when  $U_l^j(r_0) = 0$ , were also calculated and used to obtain the separate JWKB differential cross sections and their weighted average. The results for these differential cross sections at the same relative energies are shown in Fig. 2 by the dashed lines. Also shown in Fig. 2 (dotted lines) are the differential cross sections determined using the average potential,  $V_{ave}(r)$ . It is seen from these plots that at low energies small-angle scattering is not well described by either the average potential or the JWKB approximation although the latter is better. At the largest energies shown all these results roughly agree. In Fig. 3 we give the average differential cross section, at relative energies  $E = 1$  and  $10$  eV, in the form  $(d\sigma/dT)/\sigma_d$  and compare it to the simple steeply repulsive form used extensively in sputtering,  $d\sigma/dT \approx C/T$  where  $C = \sigma_d(E_0)/2$  (Sigmund, 1981; and Johnson, 1994). It is seen that the simple analytic form is reasonable at large energies and when  $T$  is not close to zero.

The momentum transfer or diffusion cross section,  $\sigma_d$ , given as a function of relative energy is illustrated in Fig. 4. This cross section has also been calculated using the exact quantum phase shifts (solid line), the semiclassical JWKB phase shifts (dashed line) and phase shifts determined using the average potential (dotted line). At higher energies, the

exact and semiclassical cross sections agree well, but at lower energies the semiclassical result becomes less accurate and exact phase shifts must be used.

Similarly, the total integrated cross sections for the exact calculations (solid line), the semiclassical calculations (dashed line) and the results of the average potential (dotted line) all as a function of relative energy are also given in Fig. 4. Again, it is seen that the differences are not large and good agreement is shown between the exact and semiclassical cross sections for energies of greater than 3 eV.

#### 4. Discussion

The elastic scattering cross sections for the  $O(^3P)+O(^3P)$  collision were determined using the method of partial waves both exactly, by numerical integration of the wave equation, and using the semiclassical JWKB approximation. It was found that differences in the integrated cross sections are not large over the full energy range. The agreement is good above about 3 eV and better for the diffusion cross section than for the total cross section. Therefore the semiclassical JWKB phase shifts, at these energies, can be considered a good approximation to the integrated cross section for this system. An average of the 18 interaction potentials required for this system was also calculated and the cross sections determined. This method yields smaller results than that of the full calculation and produces none of the structure. At higher energies ( $E > 5$  eV) the results begin to compare well. This is somewhat surprising based on earlier work (Johnson et al., 1972) and is due to the large number of differential cross sections averaged here.

For the angular differential cross section at low energies, the JWKB fails at small angles as does that cross section obtained from the average potential (Fig. 2). However, at higher energies ( $E = 10$  eV, Fig. 2) the JWKB again gives very good agreement with the exact differential cross section at all angles.

As stated in the introduction, a cross section of  $2 \times 10^{-15} \text{ cm}^2$  has been frequently used to determine the exobase column density,  $\sigma^{-1} \approx 5 \times 10^{14} / \text{cm}^2$  for an atomic oxygen thermosphere. Here we see this is close to the value of  $\sigma$  for the energy range shown. However, the differential cross sections are not isotropic as in the hard sphere models often used. The total elastic cross section,  $\sigma$ , is the quantity that should be used in Monte Carlo models for determining the mean free path to the next collision. However, this cross section is dominated by soft collisions. Therefore, the mean escape depth corresponds to a larger column density (Johnson, 1994). A reasonable estimate for non-thermal (eV) processes is  $\approx 1.3/\sigma_d$  (Johnson, 1994). This gives a larger column density varying from about  $1.0 \times 10^{15} / \text{cm}^2$  at  $E = 1$  eV to  $2.5 \times 10^{14} / \text{cm}^2$  at  $E = 10$  eV. The former applies to processes like those in Eq. (1) and the latter applies, roughly, to a sputtered atmosphere.

## Acknowledgements

This work was supported by NASA's Planetary Atmosphere Program.

## References

- Bransden, B.H., Joachain, C.J., 1983. *Physics of Atoms and Molecules*. Longman, New York.
- Chamberlain, J.W., Hunten, D.M., 1987. *Theory of Planetary Atmospheres*, Vol. 36. Academic Press, New York.
- Foreman, P.B., Lees, A.B., Rol, P.K., 1976. Repulsive potentials for the interaction of oxygen atoms with the noble gases and atmospheric molecules. *Chem. Phys.* 12, 213–224.
- Fox, J.L., Bougher, S.W., 1991. Structure, luminosity and dynamics of the Venus thermosphere. *Space Sci. Rev.* 55, 357–489.
- Gärtner, K., Hehl, K., 1979. Theoretical description of elastic atom–atom scattering. *Phys. Stat. Sol. B* 94, 231–238.
- Hunten, D.M., Donahue, T.M., Walker, J.C.G., Kasting, J.F., 1989. Escape of atmospheres and loss of water. In: Atreya, S.K., Pollack, J.B., Matthews, M.S. (Eds.), *Origin and Evolution of Planetary Atmospheres*. University of Arizona Press, Tucson, pp. 386–442.
- Joachain, C.J., 1975. *Quantum Collision Theory*. North-Holland, Amsterdam.
- Johnson, R.E., 1982. *An Introduction to Atomic and Molecular Collisions*. Plenum Press, New York.
- Johnson, R.E., 1990. *Energetic Charged Particle Interaction with Atmospheres and Surfaces: Physics and Chemistry of Space*. Springer, Berlin.
- Johnson, R.E., 1994. Plasma-induced sputtering of an atmosphere. *Space Sci. Rev.* 69, 215–253.
- Johnson, R.E., Carlston, C.E., Boring, J.W., 1972. Energy dependence in the total differential cross sections for  $H^+ + Kr$  and  $H^+ + Ar$ . *Chem. Phys. Lett.* 16, 119–122.
- Johnson, R.E., Killen, R.M., Waite, J.H., Lewis, W.S., 1998. Europa's surface and sputter-produced ionosphere. *Geophys. Res. Lett.* 25, 3257–3260.
- Konowalow, D.D., Hirschfelder, J.O., Bruno, L.J., 1959. Low-temperature, low-pressure transport coefficients for gaseous oxygen and sulfur atoms. *Chem. Phys.* 31, 1575–1579.
- Nagy, A.F., Cravens, T.E., Yee, J.H., Stewart, A.I.F., 1981. Hot oxygen atoms in the upper atmosphere of Venus. *Geophys. Res. Lett.* 8, 629–632.
- Paxton, L.J., 1985. Pioneer Venus Orbiter ultra violet spectrometer limb observations: analysis and interpretation of the 166- and 156-nm data. *Geophys. Res.* 90, 5089–5096.
- Saxon, R.P., Lui, B.J., 1977. Ab Initio Configuration Interaction Study of the Valence States of  $O_2$ . *Chem. Phys.* 67, 5432–5441.
- Sigmund, P., 1981. Sputtering by ion bombardment: theoretical concepts. In: Berisch, B. (Ed.), *Sputtering by Particle Bombardment*. Springer, Berlin, New York.
- Yee, J.H., Dalgarno, A., 1985. Energy transfer of  $O(^1S)$  atoms in collision with  $O(^3P)$  atoms. *Planet. Space. Sci.* 33, 825–830.
- Yee, J.H., Guberman, S.L., Dalgarno, A., 1990. Collisional quenching of  $O(^1D)$  by  $O(^3P)$ . *Planet. Space. Sci.* 38, 647–652.
- Zeigler, J.F., Biersack, J.P., Littmark, U., 1985. *The Stopping and Range of Ions in Solids*, Vol. 1. Pergamon Press, Oxford.
- Zhang, M.H.G., Bougher, S.W., Nagy, A.F., 1993. The ancient oxygen atmosphere of Mars: implications for atmospheric evolution. *J. Geophys. Res.* 98, 10,915–10,923.